

REMOTE DETECTION OF TURBULENCE USING GROUND-BASED DOPPLER RADARS

John K. Williams*, Larry Cornman, Danika Gilbert, Steven G. Carson, and Jaimi Yee
National Center for Atmospheric Research, Boulder, Colorado

1. INTRODUCTION

Commercial and general aviation aircraft frequently encounter unexpected turbulence that is hazardous to both aircraft and passengers. For air carriers, turbulence is the leading cause of occupant injuries, and it occasionally results in severe aircraft damage and fatalities (MCR, 1999). The cost to airlines due to injuries to flight attendants and passengers, aircraft damage, the need for additional inspections and maintenance, and associated flight delays is substantial. Moreover, encounters with even moderate turbulence may reduce passengers' confidence in airline safety. While clear-air turbulence forecasts based on numerical weather model data are now routinely generated and possess reasonable skill for levels above 21,000 ft (Sharman, 2002), a similar system for identifying and disseminating information about hazardous convectively-induced turbulence remains lacking. This omission is particularly significant because historical data suggest that over 60% of turbulence-related aircraft accidents are due to convectively-induced turbulence (Cornman, 1993).

To begin to ameliorate this deficiency, the FAA's Aviation Weather Research Program has directed the National Center for Atmospheric Research (NCAR) to develop an improved Doppler radar turbulence detection capability. The NCAR Turbulence Detection Algorithm (NTDA) makes use of the radar-measured reflectivity, radial velocity, and spectrum width to produce estimates of eddy dissipation rate (EDR), an aircraft-independent turbulence metric, along with associated quality control indices, or confidences. This fuzzy-logic algorithm, which may eventually be installed on the NEXRAD and TDWR radars that provide coverage of most of the conterminous United States, is expected to be a central component in a system that will eventually utilize radar, satellite, *in situ*, and numerical weather model data to produce a nationwide integrated turbulence detection product.

In this paper, the authors describe an experimental version of the new turbulence detection algorithm that has been implemented and verified using comparisons between archived NEXRAD data and *in situ* data from flight tests, NTSB turbulence encounter cases, and an automated turbulence reporting system operating on commercial aircraft. The verification process, while not yet comprehensive, suggests that the turbulence detection algorithm has adequate skill to be of significant operational utility, as will be shown below.

* Corresponding author address: John K. Williams, National Center for Atmospheric Research, P.O. Box 3000, Boulder, CO 80307; email: jkwillia@ucar.edu.

2. NCAR TURBULENCE DETECTION ALGORITHM

The NCAR turbulence detection algorithm (NTDA) utilizes the first three moments of the Doppler spectrum—the reflectivity, radial velocity, and spectrum width—to perform data quality control and produce EDR estimates on the same polar grid as is used for the raw moment data (see Figure 1). Data quality control is performed by computing a quality control index, or confidence, for each measurement. For example, the spectrum width confidence computation is based on the signal-to-noise ratio, or SNR (which for NEXRAD Level II data is inferred from the reflectivity and range from the radar), the value of the spectrum width, the local variance of the spectrum width field, and image processing techniques designed to identify known artifacts. The confidence values for each measurement are then propagated into the EDR computations as weights for local confidence-weighted averaging, and are also used to determine a confidence value for the resulting EDR. Three distinct methods are used for computing EDR: a second-moment method, which makes use of the measured spectrum widths; a combined first and second-moment method, which also makes use of the local variance of the radial velocity; and a structure function method, which utilizes the radial velocity measurements. The various EDR estimates, along with their associated confidences, are combined in a fuzzy-logic framework, with a single EDR and associated confidence produced for each radar measurement location. The structure of the algorithm, as implemented for NEXRAD Level II data, is diagrammed in Figure 1. For the results presented in this paper, however, only the output of the second moment module of the algorithm is used.

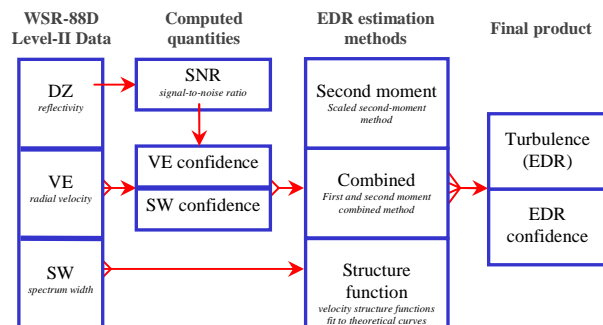


Figure 1: Diagram of the NTDA, as implemented for the WSR-88D (NEXRAD) radar. The Level II reflectivity, radial velocity and spectrum width data are used to compute EDR and an associated confidence for each radar measurement point via a fuzzy-logic framework.

3. NTDA VERIFICATION

Development, tuning, and verification of the NTDA has been performed over several years using data from research aircraft (notably the SDSM&T T-28) and Doppler research radars, including the Mile High radar and CSU CHILL radar. Recently, however, it has become possible to obtain archived NEXRAD Level II data directly from the National Climate Data Center (NCDC) via a web-based interface, making it feasible to run the NTDA for any in-cloud turbulence case in which *in situ* turbulence data are available for comparison. Sources of high-quality *in situ* turbulence data include instrumented research aircraft, flight data recorder information supplied by the National Transportation Safety Board (NTSB), and EDR values generated by an automated reporting system currently operating on a number of United Airlines aircraft (Cornman, 1995 and 2004).

3.1 NASA Flight Test Data

In the spring of 2002, a series of eleven flights were performed by the instrumented NASA Langley B-757 aircraft as part of a successful test of an airborne radar turbulence detection algorithm developed by NCAR for the NASA Aviation Safety and Security Program's Turbulence Prediction and Warning Systems project. The high-rate winds data recorded by the aircraft comprise a dataset that is also ideal for evaluating the performance of the NTDA, run on archived Level II data from NEXRAD radars along the flight paths.

The B-757's 20 Hz vertical winds data were used to estimate eddy dissipation rate (EDR), an atmospheric turbulence metric, using a single parameter maximum likelihood -5/3 model that assumes a von Karman energy spectrum form. In particular, a sliding window of width 256 points was used, with spectral frequency cutoffs set at 0.5 and 5 Hz. This temporal window size corresponds to an along-path distance of about 3 km at the aircraft's average cruising speed. In Figure 2, these computed EDR values are depicted at 30-second intervals along the flight path in for NASA flights 230 and 232, which took place on April 15 and 30, 2002, respectively. During flight 230, moderate or greater (MoG) turbulence was experienced over northern and eastern South Carolina and eastern North Carolina, and each of those encounters was in a region covered by at least three NEXRADs having available archived data. For flight 232, MoG turbulence was encountered over north-central Alabama. Although as many as five NEXRADs provide coverage of this region, three of these (KGWX, KBMX, and KMXX) had no data available from the NCDC archives.

Comparisons between the aircraft data and the results from the NTDA running on the archived radar data were performed by locating the nearest three radar sweeps in space and time to each aircraft location. These were then utilized in two ways. First, a comprehensive series of overlay plots were generated to permit comparison between the aircraft EDR and the EDR computed by the NTDA for each sweep. Two sample plots are depicted in Figure 3 and Figure 4.

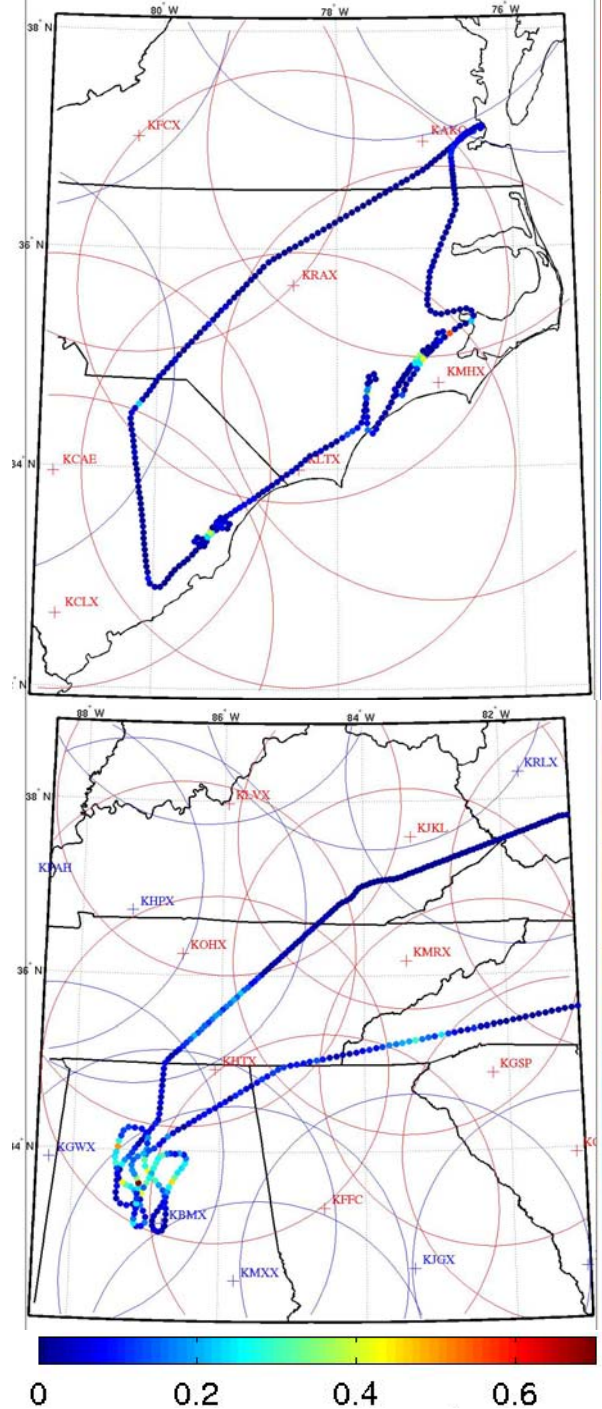


Figure 2: (Top) Flight path for NASA flight 230 on April 15, 2002, depicting EDR values scaled from 0 (blue) to 0.7 $m^{2/3}/s$ (red) at 30-second intervals. NEXRAD radar positions and 220-km range rings are superimposed, with red indicating that the radar intersected the flight path and the archived Level II data were available. The aircraft took off from Hampton, VA, and traveled counter-clockwise. (Bottom) A similar plot depicting a portion of the flight path for NASA flight 232 on April 30, 2002; the flight direction was again counter-clockwise.

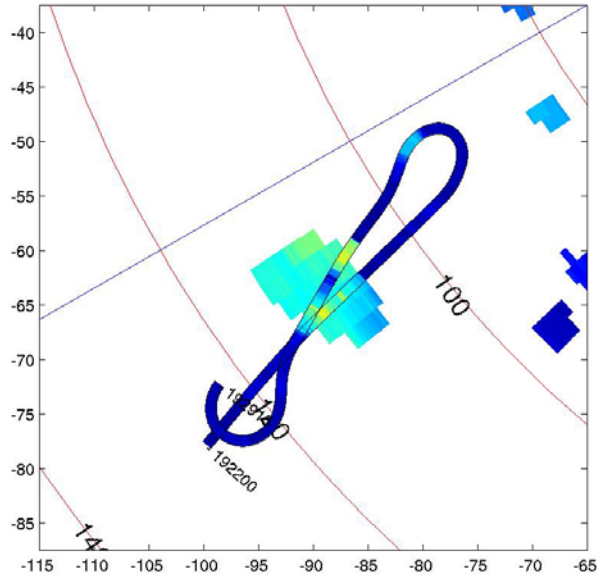


Figure 3: Overlay of *in situ* EDR values depicted along the aircraft track for NASA flight 230, 19:22:00-19:29:15, superimposed over the NTDA EDR values from the KLTX 2.4° elevation sweep beginning at 19:25:26. Both EDR values are on the same scale as Figure 2, ranging from 0 (blue) to $0.7 \text{ m}^{2/3}/\text{s}$ (red). The labels on the range rings and the axes represent the distance from KLTX, in km. The aircraft is within about 1 km of the sweep throughout this flight segment, and the radar reflectivity ranges from about 5-30 dBZ within the turbulent region.

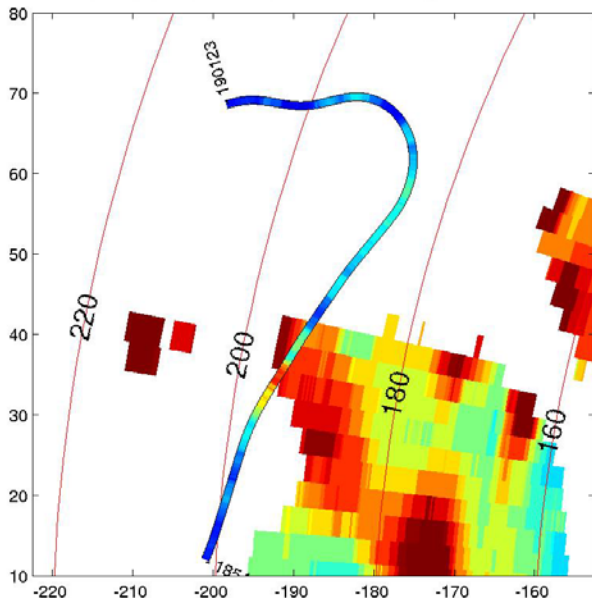


Figure 4: Identical to Figure 3, except for NASA flight 232, 18:54:51-19:01:23, and KFFC 2.4° elevation sweep beginning at 18:57:51. The aircraft is again within about 1 km of the sweep, and the radar reflectivity ranges between about 5-15 dBZ in the region where the aircraft track intersects the radar-detected turbulence “hot spot”.

Although precise collocation and quantitative matches were not achieved, both plots show that the radar successfully detected hazardous turbulence of about the right intensity in the region of the aircraft encounter. Moreover, both encounters were in regions of relatively low reflectivity ($< 30 \text{ dBZ}$ in Figure 3 and $< 15 \text{ dBZ}$ in Figure 4) where commercial aircraft commonly fly. On the other hand, no radar moments data were available near the location of the smaller MoG turbulence encounter north of the larger encounter in Figure 4; this highlights a limitation of any turbulence detection algorithm based solely on Doppler weather radar data: it is inherently unable to measure out-of-cloud turbulence.

A second level of processing was performed to extract the median reflectivity, SNR, and NTDA EDR values from a disc of radius 2 km around each aircraft location on each “nearby” radar sweep (time within 3 minutes and vertical displacement less than 3 km). The results are displayed in a series of timeseries plots for each radar depicting the radar-detected and *in situ* EDRs and reflectivity and SNR timeseries. In addition, a plot was designed to visualize the EDR values from all nearby sweeps from all appropriate radars and compare them with the aircraft EDRs. An example of such a “stacked track” plot for NASA flight 230, 20:07:10-20:12:30 is shown in Figure 5. Note that the four radars that provide coverage of this turbulence encounter generate similar EDR estimates and that these match well with the co-located *in situ* values, providing compelling evidence of the NTDA algorithm’s skill.

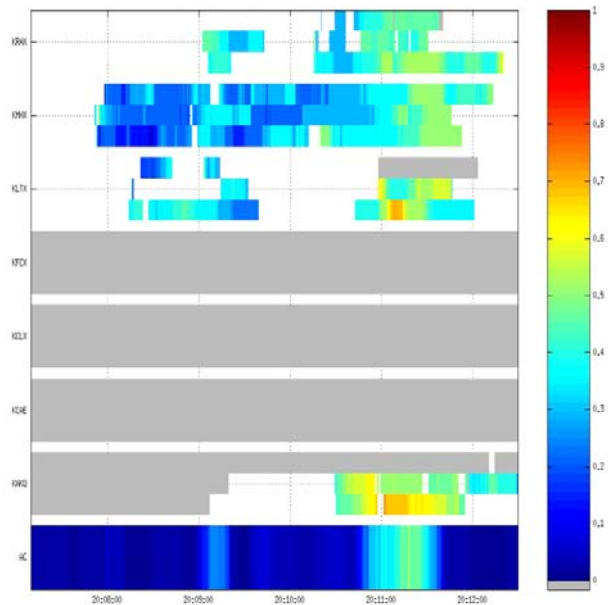


Figure 5: “Stacked track” plot for NASA flight 230, 20:07:10-20:12:30 depicting the color-scaled timeseries of aircraft EDRs (“AC”, bottom stripe) and the 2-km disc median NTDA EDRs from the three nearest sweeps of radars KAKQ, KCAE, KCLX, KFCX, KLTX, KMHX, and KRAX. Gray indicates that the radar was out of range, whereas white depicts times for which a radar sweep was within range but contained no usable data. The EDR color scale ranges from 0 to $1 \text{ m}^{2/3}/\text{s}$.

The set of timeseries, overlay, and stacked-track plots generated by the analysis described above were used to score the ability of the NTDA to detect MoG turbulence encountered by the aircraft from 55 flight segment “events” drawn from the eleven flights of the NASA flight test. A similar scoring exercise performed using the output of the airborne radar turbulence detection algorithm identified 34 correct detections, 8 misses, 4 nuisance alerts, and 9 correct nulls (Cornman, 2003), producing a probability of detection (PoD) of 81% with a nuisance alert rate of 11%. For the NTDA analysis, 15 events had no available archived NEXRAD data intersecting them. Of the remaining 40, preliminary scoring identified 32 correct detections, 2 misses, 6 nuisance alerts, and no correct nulls, yielding a PoD of 94% and a NAR of 16%. This analysis suggests that the NTDA may have skill comparable to that of the airborne radar algorithm for detecting hazardous turbulence, but that more work needs to be done to reduce the number of nuisance alerts. However, it should also be noted that research flights aimed specifically at encountering turbulence may not provide a dataset representative of the conditions encountered by commercial aircraft in an operational environment, and so care must be taken in interpreting these results.

3.2 NTSB Turbulence Encounter Cases

In addition to flight test data, high-rate accelerometer data from flight data recorders (FDRs) provide information about turbulence that can be used to verify NTDA performance, and the NTSB has provided FDR data for several turbulence-related accident cases to NCAR for that purpose. These case studies are especially compelling because they represent accidental encounters that might have been prevented by an operational turbulence detection capability. Since these accidents are still under investigation by the NTSB, these data may not yet be released publicly, and hence a full description of the results cannot be provided here. However, two severe turbulence encounter cases are described based on the times and locations of the encounters.

The first case occurred on November 17, 2002, at 23:00 UTC as a regional jet was descending near Rockville, VA (approximately 37:44 N latitude, 77:43 W longitude, and 18,000 ft) en route to Washington National Airport. Fortunately, all passengers were in their seats in preparation for landing and none were injured, though the aircraft required extensive inspection. As Figure 6 shows, the NTDA successfully detected a coherent region of persistent, very strong turbulence—eddy dissipation rates well above $1.0 \text{ m}^{2/3}/\text{s}$ —in that region, despite very low reflectivity values between 10 and 15 dBZ there. Moreover, this diagnosis was available as early as twelve minutes before the encounter, suggesting the potential efficacy of an NTDA-based tactical turbulence warning system for this case.

A second turbulence encounter case occurred on August 6, 2003 at 20:57 UTC as an Airbus A340 was at cruise altitude over Walnut Ridge, AR (approximately 36:33 N latitude, 90:42 W longitude, and 31,000 ft) en

route to Houston, TX. Figure 7 depicts the NTDA EDR values produced from the four 2.4° radar sweeps from KPAH immediately preceding the encounter time. In this case, the NTDA detected hazardous turbulence at the location of the encounter fourteen minutes in advance, and the extent and magnitude of the turbulence increased over subsequent scans. The radar reflectivity grew from about 10 to 30 dBZ at the location of the encounter during this time, but its magnitude would likely not have appeared dangerous to

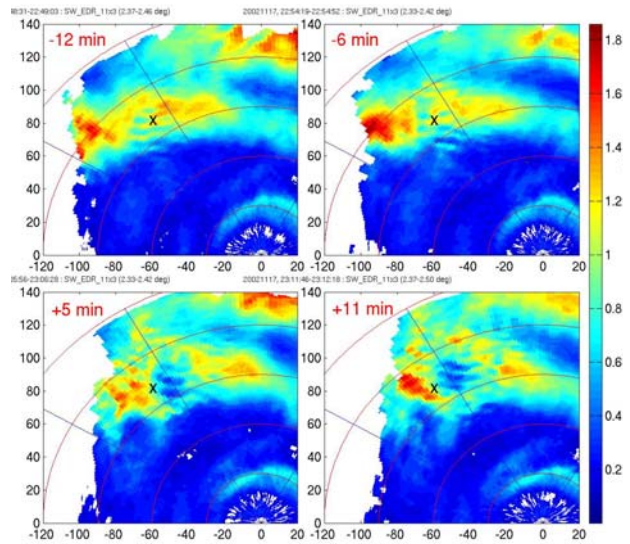


Figure 6: NTDA EDR from KAKQ 2.4° sweeps at 22:49, 22:55, 23:06, 23:12 UTC on November 17, 2002, ranging from 12 minutes before to 11 minutes after the severe turbulence encounter described in the text, which occurred at the location marked by the “X”. Note the unusually large EDR scale, from 0 to $1.85 \text{ m}^{2/3}/\text{s}$.

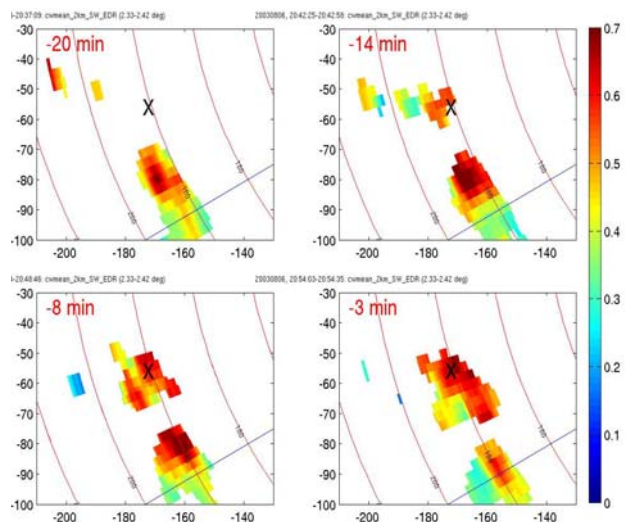


Figure 7: NTDA EDR from KPAH 2.4° sweeps at 20:37, 20:43, 20:49, and 20:54 UTC on August 6, 2003, ranging from 20 minutes to 3 minutes before the severe turbulence encounter described in the text. The EDR color scale ranges from 0 to $0.7 \text{ m}^{2/3}/\text{s}$.

the pilots. It appears that an NTDA-based turbulence warning system would have been capable of providing adequate warning for this case, and thus possibly prevented the 43 minor injuries, two serious injuries, and minor damage to the aircraft that resulted from the unexpected turbulence encounter. However, the quickly-evolving nature of convective turbulence illustrated by this case will require that the latency between the radar measurement and the communication of the turbulence hazard to the pilot be very small for the warnings to be effective.

3.2 *In situ* Turbulence Reports

While FDR data cases like those described above provide valuable information on hazardous turbulence encounters, the number of events is insufficient to draw statistically meaningful conclusions. On the other hand, the Cornman *in situ* turbulence algorithm (Cornman, 1995 and 2004) is currently installed on about 200 United Airlines B-737 and B-757 aircraft, and efforts are underway to deploy it on additional aircraft types and airlines in the near future. The *in situ* algorithm provides median and peak EDR values reported at intervals of one minute or less, thereby supplying a large dataset of objective turbulence measurements in locations and conditions where aircraft commonly fly. When an automated method to quality control these data is completed, several hundred flight hours per day of *in situ* turbulence information will be available for use in comparing to NTDA-derived values and producing a comprehensive statistical analysis.

An illustration is provided using a segment from a flight from Chicago to Salt Lake City that began just after midnight UTC on November 18, 2003. Figure 8 and Figure 9 depict the peak *in situ* EDR measurements obtained from the automated reporting algorithm, represented by colors in circles along the flight path as the aircraft flew from east to west across Iowa and western Nebraska. In Figure 8, the aircraft track is overlaid on the radar-measured reflectivity at 31,000 ft—the average cruising altitude for the flight—obtained by merging data from the KLNx, KUEx, KOAX, KDMx, KDVN and KILx NEXRADs onto a 2 km x 2 km x 2,000 ft grid. Three distinct instances of elevated *in situ* EDRs may be observed: 00:11 - 00:12 over east-central Iowa, 00:27 - 00:33 over western Iowa, and 00:46 - 00:48 UTC over northeastern Nebraska. The valid time of the radar analysis is 00:30, meaning that it used radar sweeps collected between 00:24 and 00:30. At that time, which coincides with the second turbulence encounter, the radar-measured reflectivity was less than 10 dBZ along the flight path. This implies that the cloud would not have been visible on an airborne radar display, although the pilots appear to have been deviating around a more intense echo further south. The merged confidence-weighted mean NTDA EDRs shown in Figure 9 show a good match with the beginning of this turbulence encounter, although the last and most intense part occurred out of cloud and hence no direct EDR measurement was possible. This case suggests the importance of developing diagnostics for EDR in the vicinity of convection to augment the direct in-cloud turbulence detection capability.

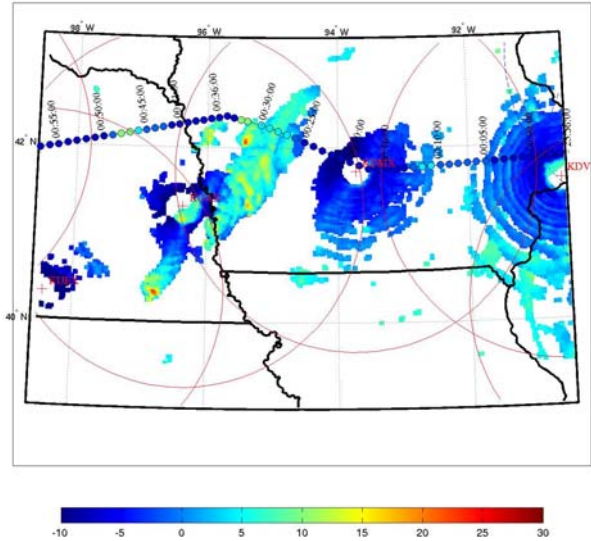


Figure 8: Automated *in situ* reports of peak EDR over 1-minute segments from a flight from Chicago to Salt Lake City on November 18, 2003, represented as colored circles scaled from 0 (blue) to $0.7 \text{ m}^{2/3}/\text{s}$ (red). The flight track is overlaid on the radar reflectivity at 31,000 ft obtained from merging data from the KLNx, KUEx, KOAX, KDMx, KDVN, and KILx NEXRADs recorded between 00:24 and 00:30 UTC and gridding them onto a 2 km x 2 km x 2000 ft grid. The reflectivity scale, shown below the plot, ranges from -10 to 30 dBZ.

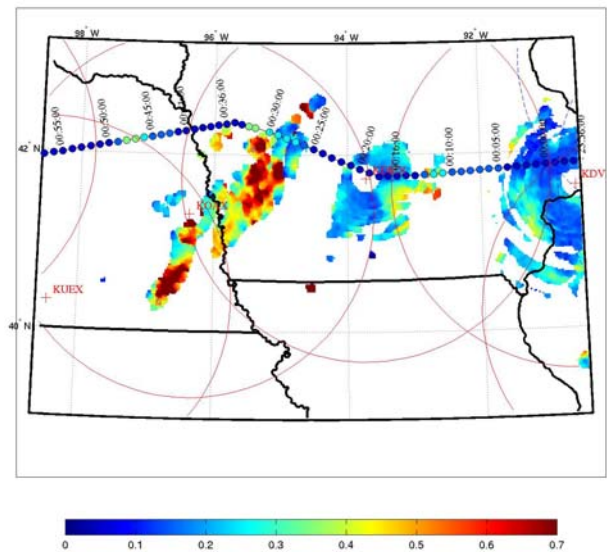


Figure 9: Identical to Figure 8 but with the aircraft track overlaid on the NTDA EDRs at 31,000 ft obtained by performing confidence-weighted averaging of the values recorded by the KLNx, KUEx, KOAX, KDMx, KDVN, and KILx NEXRADs between 00:24 and 00:30 UTC. Both the *in situ* and NTDA-derived EDRs are represented on a color scale from 0 to $0.7 \text{ m}^{2/3}/\text{s}$.

4. CONCLUSION

A new Doppler radar turbulence detection algorithm, the NTDA, utilizes the radar reflectivity, radial velocity, and spectrum width data to perform quality control and produce EDR estimates. Initial verification studies using archived Level II data and *in situ* data from flight tests, NTSB turbulence encounter cases, and automatically-reported EDR data from commercial aircraft suggest that the NTDA has skill in detecting hazardous turbulence and has the potential to be a valuable new input to decision support systems that help pilots, air traffic controllers, and dispatchers assess weather-related aviation hazards. In particular, this capability could improve safety, passenger confidence, and air traffic flow during convective events.

It is anticipated that the NTDA will eventually be implemented on all NEXRAD and TDWR radars so that the EDRs it produces will be readily available to all potential users for operational or scientific purposes. In addition, NCAR has requested funding from the FAA's Aviation Weather Research Program to develop a real-time turbulence detection product based on the NTDA EDRs and confidences that will support the unique needs of the aviation community. A web-based product is foreseen that will provide a nationwide, gridded turbulence diagnosis display for specified flight levels, thereby supplementing the upper-level turbulence forecasts currently supplied by the Graphical Turbulence Guidance product on the National Weather Service Aviation Weather Center's Aviation Digital Data Service (ADDS). Eventually, the NTDA output will be combined with satellite, *in situ*, and numerical weather prediction model data to identify and forecast regions of hazardous turbulence.

5. ACKNOWLEDGEMENTS

The authors wish to thank the National Transportation Safety Board for supplying Flight Data Recorder information for the case studies described herein, and the NASA Aviation Safety and Security Program and Langley Research Center for providing aircraft data from the spring, 2002 TPAWS flight tests.

This research is in response to requirements and funding by the Federal Aviation Administration (FAA). The views expressed are those of the authors and do not necessarily represent the official policy or position of the FAA.

6. REFERENCES

- Cornman, L. B. and B. Carmichael, 1993: Varied research efforts are under way to find means of avoiding air turbulence. *ICAO Journal*, 48, 10-15.
- Cornman, L. B., C. S. Morse, and G. Cuning, 1995: Real-time estimation of atmospheric turbulence severity from in-situ aircraft measurements, *Journal of Aircraft*, 32, 171-177.
- Cornman, L. B., J. Williams, G. Meymaris, and B. Chorbajian, 2003: Verification of an Airborne Radar Turbulence Detection Algorithm. *6th International Symposium on Tropospheric Profiling: Needs and Technologies*, 9-12.
- Cornman, L. B., G. Meymaris and M. Limber, 2004: An update on the FAA Aviation Weather Research Program's *in situ* turbulence measurement and reporting system. *11th AMS Conference on Aviation, Range, and Aerospace Meteorology*.
- MCR Federal, Inc., "Turbulence Benefits Analysis. Historical Safety Impact of Turbulence." BR-7100/010-1, 9 June 1999.
- Sharman, R., C. Tebaldi, J. Wolff and G. Wiener, 2002: Results from the NCAR Integrated Turbulence Forecasting Algorithm (ITFA) for predicting upper level clear-air turbulence. *10th AMS Conference on Aviation, Range, and Aerospace Meteorology*, 351-354.